Fluorescence Decay and Spectral Evolution in Intact Photosystem I of Higher Plants

Roberta Croce,[‡] Dieter Dorra,[§] Alfred R. Holzwarth,[§] and Robert C. Jennings*[,‡]

Dipartimento di Biologia and Centro CNR Biologia Cellulare e Molecolare delle Piante, Universitá di Milano, Via Celoria 26, 20133 Milano, Italy, and Max-Planck-Institüt für Strahlenchemie, Stifstrasse 34-36, 45470 Mülheim an der Ruhr, Germany

Received November 17, 1999; Revised Manuscript Received March 22, 2000

ABSTRACT: A photosystem I preparation from maize, containing its full antenna complement (PSI-200) and in which detergent effects on chlorophyll coupling are almost completely absent, has been studied by time-resolved fluorescence techniques with ∼5 ps resolution at 280 and 170 K in the wavelength interval of 690−780 nm. The data have been analyzed in terms of both the decay-associated spectra (DAS) and the time-resolved emission spectra (TRES). As in a previous room temperature study [Turconi, S., Weber, N., Schweitzer, D., Strotmann, H., and Holzwarth, A. R. (1994) *Biochim. Biophys. Acta 1187,* 324−334], the 280 K decay is well described by three DAS components in the 11−130 ps time range, the fastest of which displays both positive and negative amplitudes characteristic of excitation transfer from the bulk to the red antenna forms. Both the 57 and 130 ps components have all positive amplitudes and describe complex decay and equilibration processes involving the red forms. At 170 K, four major components in the 10−715 ps time range are required to describe the decay. The fastest represents bulk to red form transfer processes, while the 55, 216, and 715 ps decays, with all positive amplitudes, have maxima near 720, 730, and 740 nm, respectively, in accord with previous steady-state fluorescence measurements. The width and asymmetry of these DAS indicate that they are spectrally complex and represent decay and equilibration processes involving the red forms. Spectral evolution during the fluorescence decay process was analyzed in terms of the TRES. The red shifting of the TRES was analyzed in terms of the first central spectral moment (mean spectral energy) which is biexponential at both temperatures. The slower component, which describes equilibration between the red forms, leads to spectral red shifting during the entire fluorescence decay process, and the mean lifetimes of the spectral moments at 280 and 170 K (86 and 291 ps, respectively) are similar to the mean lifetimes of the fluorescence decays (119 and 384 ps, respectively). Thus, both spectral evolution and the trapping-associated fluorescence decay occur on a similar time scale, and both processes display a very similar temperature sensitivity. On the basis of these data, it is concluded that trapping in PSI-200 is to a large extent rate-limited by excitation diffusion in the antenna and in particular by the slow "uphill" transfer from the low-energy forms to the bulk and/or inner core chlorophyll molecules.

The photosynthetic electron transport system of higher plants carries electrons from water to NADP against an electrochemical gradient of about 1.2 V. The free energy for this process comes from light absorption at the level of two distinct photosystems known as photosystem I and photosystem II. In both photosystems, light is absorbed by a large array of antenna pigments, mostly chlorophylls, and subsequently transferred on a picosecond time scale to reaction centers where primary photochemical trapping occurs. In the case of PSI,[1] two physically separate moieties are distinguishable (for review, see ref *3*). (i) A core complex which in addition to the special reaction center chlorophyll pair, P700, and the primary electron acceptors, also binds about 90 antenna chl *a* molecules. A quite detailed crystallographic structure at 4.5 Å resolution has been recently proposed for the core complex of a cyanobacterium (*4*) in which more than 80% of the chls are identified. The average interchromophore distance between antenna molecules is 11−12 Å, while P700 seems to be located in a region of low chromophore density except for a group of six pigments which include the primary electron acceptor and accessory chls. (ii) Peripheral antenna complexes (LHCI) collectively bind more than 100 chl *a* and/or *b* molecules. Four different LHCI complex polypeptides have been identified which are arranged around the core (*5*) as dimers, of which there are four or five per photosystem (*6*).

A characteristic of particular interest in PSI is the presence of a number of pigment pools which are energetically well separated. Thus, while the main, rather broad absorption band associated with bulk antenna pigments has its maximum near 680 nm, a number of minor, red-absorbing spectral forms are present at wavelengths longer than that of P700. The importance of these red spectral forms in understanding energy transfer pathways in PSI has been underlined in recent years by the demonstration that RC trapping at RT proceeds

* To whom correspondence should be addressed: Dipartimento di Biologia, Universitá degli Studi di Milano, Via Celoria 26, Milano, Italy. Telephone: 0039 02 26604422. Fax: 0039 02 26604399. E-mail: Robert.Jennings@unimi.it.

‡ Universitá di Milano.

§ Max-Planck-Institüt für Strahlenchemie.

[1] Abbreviations: Chl, chlorophyll; DAS, decay-associated spectra; LHCI, light-harvesting complex of PSI; PS, photosystem; PSI-200, photosystem I with full antenna complement; SAS, species-associated spectra; TRES, time-resolved emission spectra; RT, room temperature.

10.1021/bi992659r CCC: $19.00
Published on Web 05/05/2000

from a state in which most excited states are associated with the red forms both in core particles (*1*, *7*, *8*) and in PSI with its full antenna complement (PSI-200; *1*, *2*). In the case of PSI-200, it has been demonstrated that between 80 and 90% of excited states are associated with the red spectral forms in the steady state at RT (*2*). These observations clearly indicate that energy transfer from the antenna to P700 must involve thermally promoted (energetically uphill) transfer processes.

It is often reported that two red-absorbing pigments are present in PSI from plants with emission maxima near 720 and 735 nm (*9*−*12*). This may however be a somewhat simplified view as there is evidence that the 735 nm emission band reported in these studies is the unresolved sum of at least two spectral pools with fluorescence maxima near 730 and 740 nm (*2*, *13*). The stoichiometry of the 720, 730, and 740 nm pools was suggested to be six, three, and one molecule, respectively, per 200 antenna chls (*2*). While the 740 nm form is the lowest-energy emittor so far demonstrated in plant PSI, the core antenna of some cyanobacteria possesses a fluorescence band near 760 nm (*14*).

A detailed understanding of energy transfer in PSI requires kinetic studies in the picosecond and sub-picosecond time range. While a substantial body of experimental information is available for core particles, mainly prepared from cyanobacteria (*15*−*17*), less detail has been published for intact PSI-200 (*16*−*18*). A detailed study of intact PSI is particularly interesting as the 735 nm emission pool, which as pointed out above is probably an unresolved mixture of 730 and 740 emissions, seems to be associated predominately with the peripheral antenna complexes known collectively as LHCI (*9*, *19*, *20*). The early fluorescence decay studies of Mukerji and Sauer (*13*) demonstrated complex dynamics with four to five kinetic components present at room temperature and 77 K, the fastest of which had a lifetime of around 50 ps. Subsequently, Turconi et al. (*1*) demonstrated a much faster (6−14 ps) bulk antenna red form transfer component, in close agreement with the so-called equilibration component detected by several groups in core particles (*21*, *22*). In their room-temperature analysis, Turconi et al. (*1*) also detected two decay components with lifetimes in the 40−50 and 120−130 ps range. The decay-associated fluorescence spectra of both components are maximal in the emission region of the red spectral forms, with the longer-lived component being the most red-shifted. These components were both assigned to primary photochemical trapping with the lifetime and spectral differences being attributed to PSI particles with significantly different antenna sizes and red spectral form composition. In this paper, the problem of the multiple fluorescence decay components in PSI-200 has been further examined with the idea of minimizing effects due to particle heterogeneity. To this end, we have analyzed a preparation for which a thermodynamic analysis of steady-state absorption and fluorescence spectra (*2*) suggested a substantial degree of particle homogeneity (*23*). The fluorescence decay kinetics were measured and analyzed globally between 80 and 300 K in the 680−770 nm wavelength interval, which allowed a clear description of the time-resolved emission spectra and the multiple, decay-associated spectra.

An important question concerning energy trapping is whether the overall rate of primary charge separation is determined largely by the rate of excitation diffusion in the antenna (diffusion-limited) or by the rate processes which occur at or very close to the primary donor (trap-limited). The most generally accepted view favors the trap-limited situation (for review, see ref *24*) though there is little very recent data on this. In the case of PSI, this idea is based on the presence in both core particles and PSI-200 of a transfer component (5−12 ps) in fluorescence decay experiments which is much faster than trapping (50−100 ps; *1*, *7*, *8*). The fast transfer component involves excitation flow from the bulk chlorophylls to the red forms and has been interpreted as representing excitation equilibration within the antenna. Thus, trapping is envisaged to occur from a thermalized state in which superfast antenna processes do not significantly determine the overall trapping rate. In the study presented here, we specifically address this aspect by calculating the first central moment of the time-resolved emission spectra and comparing it with that of trapping at 280 and 170 K. We observe that both processes occur with similar dynamics and display similar temperature sensitivities. The data are discussed in terms of energy trapping which is mainly diffusion-limited.

MATERIALS AND METHODS

Purification of PSI-200. The complex was prepared from maize as previously reported (*2*).

Absorption and Fluorescence Spectroscopy. The steady-state absorption and fluorescence emission spectra were measured at 6 °C using an EG&G OMAIII instrument (model 1460) with an intensified diode array (model 1420) mounted on a spectrograph (Jobin-Yvon HR320). The conditions were the same as those previously reported (*2*)

Time-Resolved Fluorescence. Picosecond time-resolved fluorescence was measured by the single-photon-timing technique, using a synchronously pumped, cavity-dumped dye laser as described previously (*25*) with a repetition rate of 800 kHz and DCM as the laser dye. The overall system prompt response was typically 35 ps (fwhm). The sample was diluted in 60% glycerol and 10 mM Tricine (pH 7.8) to a final concentration of 50 μg/mL. The measurements were performed with a 1 mm cuvette in the presence of an oxygen scavenger system (glucose/glucose oxidase/catalase) to avoid oxygen effects, and the sample was changed after 1 h. The emission decays were recorded every 10 nm between 690 and 770 nm and analyzed both by single-decay and by global analysis methods (*25*, *26*).

RESULTS

Steady-State Spectra. The steady-state absorption and fluorescence spectra of the OGP-solubilized PSI-200 preparation used in this study at 280 and 170 K are presented in Figure 1A,B. They are very similar to those previously reported for this preparation (*2*) with the absorption maximum near 680 nm and the RT emission maximum at 722 nm, which shifts to 735 nm at 170 K. The fluorescence shoulder near 685 nm is associated with the bulk chlorophylls, and its magnitude decreases drastically upon lowering the temperature, as is expected on thermodynamic grounds for a well-coupled system. At 80 K, it is almost absent (unpublished data). These temperature effects on the shorter-wavelength emission band demonstrate that the sample is essentially free of uncoupled chlorophylls. We emphasize

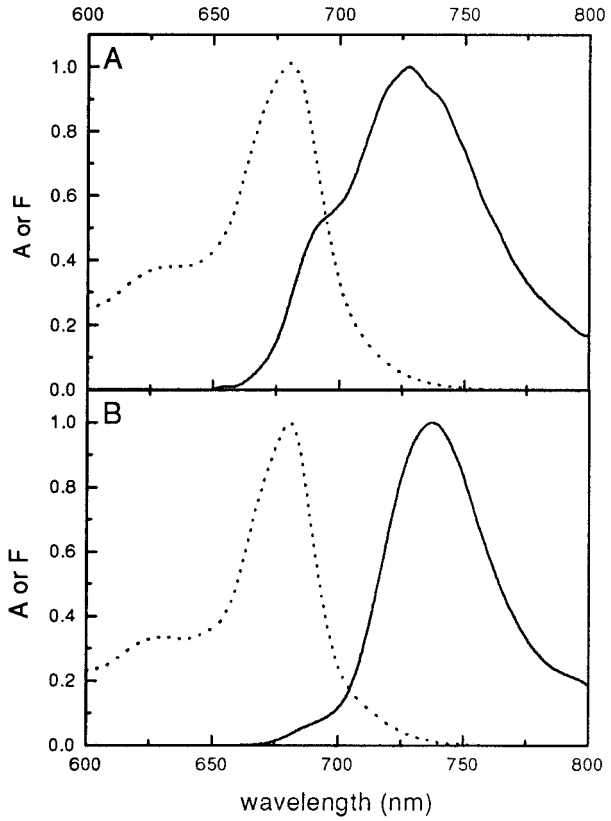

FIGURE 1: Steady-state absorption and emission spectra measured at 280 (A) and 170 K (B) of the PSI-200 preparation. Measurements were performed in the absence of added detergent.

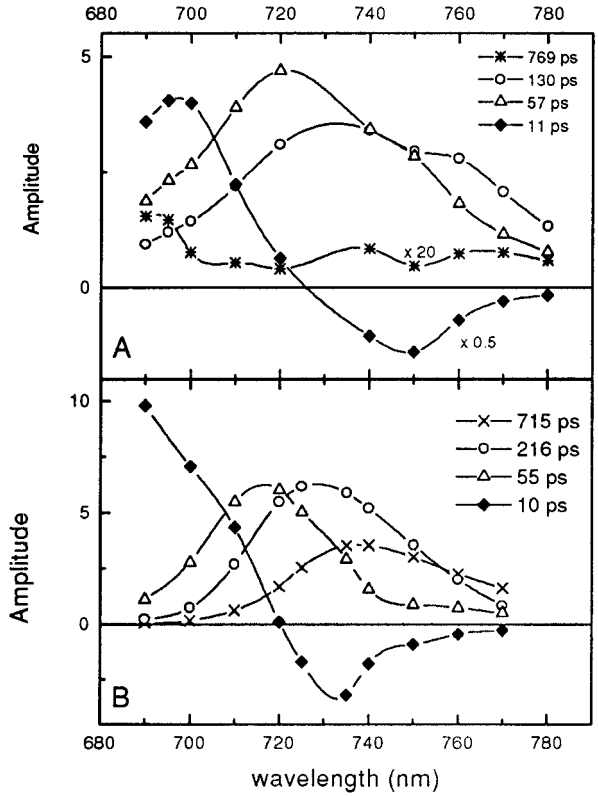

FIGURE 2: Decay-associated spectra (DAS) of the PSI-200 preparation measured at 280 (A) and 170 K (B). The decay times and the rescaling factors are indicated on the figures.

that all measurements presented in this study were performed in the absence of added detergent, as this, even at very low concentrations, causes chlorophyll uncoupling (*2*).

Time-Resolved Measurements. Time-resolved measurements were taken at several temperatures between 280 and 80 K, though we present data only for 280 and 170 K as these are sufficient to illustrate the main points. The excitation wavelength was 670 nm, and decays were recorded at eight wavelengths between 690 and 770 nm. Data were analyzed by a global analysis procedure applied to complete sets of decay measurements, and the qualities of the fits were evaluated by χ^2 and weighted residual plots. At both 280 and 170 K, four exponential lifetime components τ_i ($i = 1-4$) were required to adequately describe the decays.The DAS for these components are shown in Figure 2. The fastest component, τ_1 (10−13 ps), displays the characteristic positive and negative amplitudes of an energy transfer process for transfer from the bulk chlorophylls to the red forms and is similar to components measured previously in both large and small PSI (*1*). The decay time is insensitive to temperature within experimental error, though minor spectral changes occur. The second component has a decay time of 53−57 ps and a DAS with a maximum near 720 nm and has only positive amplitudes. Its decay time is temperature-insensitive, and there is considerable band narrowing at 170 K. The third component, τ_3 (130−216 ps), also with only positive amplitudes, has a broad maximum in the 730−740 nm interval at RT and near 740 nm at 170 K. At 280 K, its DAS is much more asymmetrical toward long wavelengths than at 170 K, suggesting a greater spectral complexity for this component at the higher temperature. This component displays a marked temperature sensitivity, slowing down at lower temperatures. The fourth component, τ_4 (715−760 ps), clearly represents different processes at 280 and 170 K. At 280 K, it is extremely weak and has all positive amplitudes with a maximum near 680 nm. We do not think that this represents completely uncoupled chlorophylls, as they usually have a 2−4 ns lifetime (*1*). In addition, this component is not seen at lower temperatures when emission from uncoupled chlorophylls should, in principle, be more easily observable due to the red shifting of antenna emission. This component may arise from a small population of weakly coupled bulk chlorophylls, which are still capable of transferring energy slowly to the antenna. On the other hand, at 170 K the τ_4 decay has a broad DAS maximum near 740 nm, which apparently has no RT equivalent. We think it is likely, however, that this 740 nm spectral component is present at room temperature in the long-wavelength wing of the markedly asymmetric 130 ps decay. At 80 K, this 740 nm DAS is resolved into two processes with maxima slightly above and slightly below 740 nm (data not presented).

To analyze spectral evolution, we have calculated the time-resolved emission spectra (TRES), from the DAS, over a time interval that corresponds to the fluorescence decay (Figure 3). The long-lived RT component, probably due to weakly coupled chlorophylls, was omitted from these calculations. The TRES corresponding formally to zero time is maximal near 700 nm and clearly also possesses considerable intensity at longer wavelengths. This indicates that significant spectral evolution occurs within the time resolution of the instrument (3−4 ps) with transfer from the bulk pigments, which were initially excited, into lower-energy

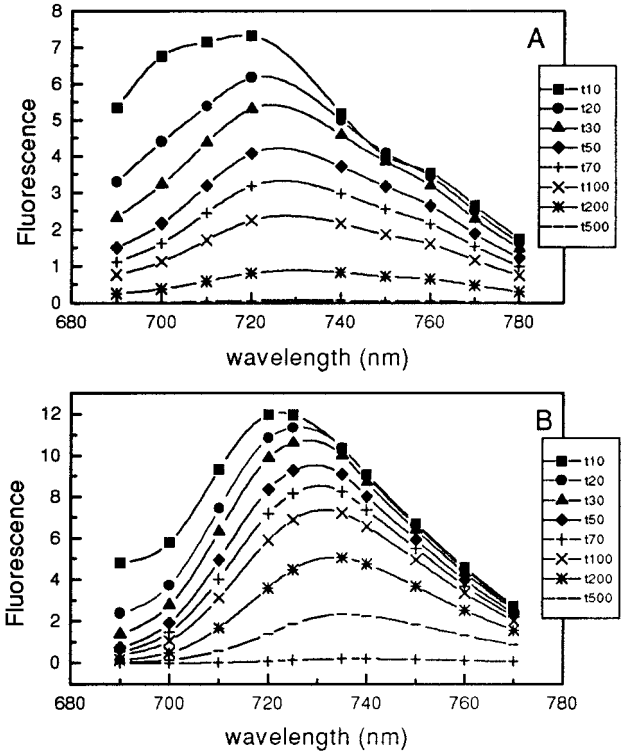

FIGURE 3: Time-resolved emission spectra (TRES) calculated from the 280 and 170 K DAS for the PSI-200 preparation. For the 280 K TRES, the long-lived (769 ps), low-amplitude, component was excluded from the calculation. TRES are shown for times of 10, 20, 30, 50, 70, 100, 200, and 500 ps which are ordered according to their decreasing amplitudes.

forms. Inspection of the TRES shows that spectral evolution toward the red occurs *continuously* right across this time interval, accompanying the excited-state decay. This observation is important as it indicates that trapping cannot be considered to occur from a thermalized state and is thus in contradiction with the trap-limited notion. To analyze this further, it is necessary to express the time development of spectral changes in quantitative terms and compare it with the dynamics of trapping. To this end, we have calculated the first-order spectral moment [$S_{1(\nu)}$] of the TRES presented in Figure 3, according to eq 1.

$$S_{1(\nu)} = \int \nu\, F(\nu)\, \mathrm{d}\nu \qquad (1)$$

This, as pointed out by Eadie et al. (*27*), yields the mean energy with respect to the spectral distriburtion $F(\nu)$. In a complex, multicomponent, spectrum, where $F(\nu) = \Sigma A_k\, f(\nu)_k$, $S_{1(\nu)}$ may be expressed as the area-weighted sum of the first-order moments of the single components [$S_{1(\nu)k}$ in eq 2] where the area ($S_{0,k}$) is the zero-order moment of each component.

$$S_{1(\nu)} = \sum S_{1(\nu)k} / \sum S_{0,k} \qquad (2)$$

Thus, $S_{1(\nu)}$ is a defining characteristic of a multicomponent spectral distribution. In the case of the TRES presented in Figure 3, where the spectral shape displays time-dependent changes, $S_{1(\nu)}$ is a parameter which describes this spectral evolution. We wish to emphasize that while $S_{1(\nu)}$ does not define a unique set of zero- and first-order moments, i.e., the same mean energy value may be given by many

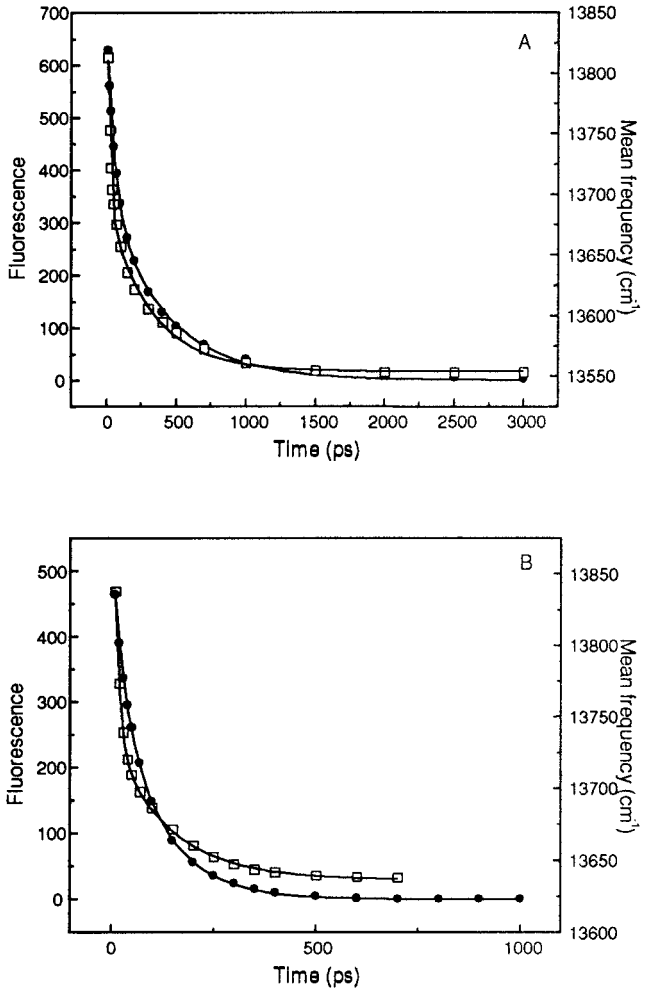

FIGURE 4: Dynamics of the mean spectral frequency (first spectral moments) of the TRES and of the total fluorescence decay calculated from the integrated TRES areas at 170 (A) and 280 K (B) for the PSI-200 preparation. Curves are the biexponential fits (see the text for details).

combinations (eq 2), this does not modify either its physical meaning as the mean spectral energy or its usefulness in describing spectral evolution.

In Figure 4, the dynamics of spectral evolution are represented in terms of the mean energy (first central moment) of the TRES calculated over the energy interval used in the time-resolved fluorescence measurements. For experimental reasons, the spectra do not go to zero at both extremities. While this is expected to be of little importance for the long-wavelength range, as above 770 nm only vibrational bands are present, it is more serious for the short-wavelength range. Thus, the $S_{1(\nu)}$ values for the early times will be biased toward lower energies. This point is further discussed below. Analysis of the data in Figure 4 shows that the excitation equilibration process is biphasic and is well approximated by two exponential curves at both 170 and 280 K (at 170 K $A_1 = 203$, $\tau_1 = 20$ ps, $A_2 = 138$, and $\tau_2 = 316$ ps and at 280 K $A_1 = 248$, $\tau_2 = 13$ ps, $A_2 = 99$, and $\tau_2 = 139$ ps, where the amplitudes refer to the total amount of spectral shifting in cm^{-1}). The fast equilibration process (EP) is clearly associated with the 10−11 ps DAS component and represents the movement of excited states from the bulk antenna to the red spectral regions. Thus, the above-mentioned bias of the initial $S_{1(\nu)}$ values toward lower

Table 1: First Central Moment of the Time Distribution of the Total Fluorescence Decay (690−770 nm) and the Mean TRES Frequency Evolution at 280 and 170 K

	280 K	170 K
fluorescence decay	99 ps	384 ps
mean frequency	86 ps	291 ps

energies does not seem to greatly influence the τ_1 of spectral evolution determined in this way. The longer-lifetime EP represents equilibration processes between the red forms, particularly those emitting near 730 and 740 nm, as can be clearly seen by inspection of the 170 K DAS (Figure 2B) where the 720 nm-associated decay is approximately complete in 150 ps. It is this component, accounting for about 30% of the spectral shifting at both temperatures, which leads to the slow overall spectral equilibration. Interestingly, it is the slow EP which displays the greater temperature sensitivity, as judged by its "yield" term ($A_n\tau_n$).

In Figure 4, the total fluorescence decays, determined from the TRES areas at different decay times $\{\int[F(\lambda)\ d\lambda]_t\}$, are presented. We emphasize that this is the total excited-state decay of the system for the 80 nm spectral interval examined and thus to a good approximation represents the dynamics of excited-state depopulation by primary photochemistry. At both temperatures, this process is well described by a biexponential decay (at 170 K $A_1 = 335$, $\tau_1 = 56$ ps, $A_2 = 346$, and $\tau_2 = 427$ ps and at 280 K $A_1 = 183$, $\tau_1 = 26$ ps, $A_2 = 370$, and $\tau_2 = 107$ ps, where the amplitudes are in arbitrary fluorescence units). Comparison of these decay components with those for the mean spectral frequency at both temperatures indicates that while the initial phase of spectral equilibration is 2−3 times faster than the fluorescence decay this is not the case for the second, slower component. At 280 K, τ_2 for spectral evolution is actually greater than for the excited-state decay. It is therefore clear from these data that the two processes of trapping and exciton dynamics cannot be considered to be occurring on very different time scales.

To directly compare the dynamics of trapping with spectral equilibration, we have calculated the first central moment of the time distribution for both the overall fluorescence decay and the mean TRES frequency evolution (Table 1). This parameter, defined in eq 3, has the physical meaning of the mean time of the process being investigated.

$$S_{1(t)} = \int t\, F(t)\, dt \tag{3}$$

and by analogy with eq 2, for a multicomponent process, $S_{1(t)}$ is given by eq 4.

$$S_{1(t)} = \sum S_{1(t)k} / \sum S_{0,k} \tag{4}$$

and is therefore calculated as $\Sigma A_k\tau_k^2/\Sigma A_k\tau_k$.

Thus, $S_{1(t)}$ is a defining characteristic of a multicomponent, time-dependent, process. Thus, for different multicomponent, time-dependent, processes (trapping and spectral evolution), it is a useful means of determining whether their dynamics are similar. From the results of this analysis (Table 1), it is evident that at both temperatures spectral evolution and the trapping-associated fluorescence decay occur on a similar time scale.

DISCUSSION

In this study, data are presented on the picosecond fluorescence decay kinetics of a large and apparently intact PSI particle binding the full complement of antenna pigments (PSI-200). Because of the mild detergent solubilization procedure that was employed and particle resuspension in the absence of added detergent, uncoupled chlorophylls seem to be virtually absent. Data have been analyzed in terms of both the DAS and TRES, which will be discussed separately.

The DAS determined at RT have three major exponential components with lifetimes and spectral characteristics which are similar, but not identical, to those previously published for a large PSI particle called PSI-110 (*1*). The fastest detected component, τ_1 (10 ps here and 14 ps in Turconi et al.), shows bulk and red form transfer characteristics as discussed by those authors. The other decay processes (τ_2 and $\tau_3 \cong 50$ and 130 ps in both studies, respectively) have their maximum amplitudes near 720 and 730−740 nm in both studies. However, in the case of the previous analysis (*1*), both of these DAS also exhibit strong emission bands in the 680−690 nm interval, characteristic of the bulk chlorophylls. These are largely absent in the PSI-200 particle used in this analysis. We interpret the presence of these short-wavelength bands in Turconi et al. (*1*) as being due to the presence of a small number of somewhat weakly coupled bulk chlorophylls due to the detergent treatment that was used and suggest that the DAS presented here may be somewhat more accurate.

In PSI-200, the RT decay processes ($\tau_2 = 57$ ps and $\tau_3 = 130$ ps) are markedly asymmetrical toward the red with the slower component displaying the greater asymmetry. This is indicative of a substantial emission heterogeneity which is at least in part resolved in the 170 K measurements where three long-wavelength DAS are detected, with maxima near 720, 730, and 740 nm. These maxima coincide with the wavelength positions of the red-emitting forms previously detected by steady-state fluorescence measurements of PSI-200 (*2*). As the DAS peaking near 740 nm is strongly asymmetrical toward longer wavelengths, we expect that small amounts of even more red-shifted chlorophylls probably occur in PSI-200. Gaussian analysis of the red emission tail of this particle at 75 K (*2*) indicates that a 760 nm emission could be present, possibly similar to the well-documented 760 nm emission in the PSI core of Spirulina (*14*), though at the moment more direct evidence for this is lacking.

In the previous RT study by Turconi et al. (*1*), the presence of only one component with clear transfer characteristics (τ_1) and two with all-positive amplitudes (τ_2 and τ_3) was explained in terms of sample heterogeneity, i.e., in terms of two types of PSI particles with different antenna content. Thus, τ_2 and τ_3 were considered to be the final decays of two separate and spectrally equilibrated systems, each with a fast transfer (equilibration) component and a slow relaxation process. This interpretation seemed most reasonable on two counts. (1) As already discussed by Suter et al. (*28*) and Trinkunas and Holzwarth (*29*), only the slowest DAS is expected to have positive amplitudes at all wavelengths. (2) The τ_2 and τ_3 DAS of Turconi et al. (*1*) have a clear structure around 690 nm, in addition to the long-wavelength signal, thus suggesting relaxation in PSI particles containing both

bulk and red form antenna chlorophylls. Concerning this latter point, we would point out that the measurements of Turconi et al. (*1*) were performed in the presence of detergent concentrations which were subsequently demonstrated to lead to the partial uncoupling of chlorophylls which then fluoresce near 690 nm (*2*). In this analysis using a PSI-200 particle prepared by mild detergent fractionation and resuspended in the absence of detergent, this 690 nm structure in the τ_2 and τ_3 DAS is almost absent with nearly all the DAS amplitude being associated with the red forms. In addition, it is demonstrated that at 170 K three DAS components with all positive amplitudes are present, with clear maxima near 720, 730, and 740 nm. In the particle heterogeneity scenario, this would suggest the presence of three types of PSI particles, each containing substantially different red pigment pools. While we cannot formally exclude this possibility, it seems rather improbable and is furthermore inconsistent with the TRES analysis in which a slow, temperature-sensitive, spectral equilibration process has been identified which apparently involves excitation movement between the red forms. This latter aspect is further discussed below.

If the all-positive DAS are not to be associated with the relaxation decays of spectroscopically different particles, they must then represent excitation equilibration processes within single PSI-200 complexes. This clearly raises the problem of the absence of negative amplitudes in these DAS. A proper discussion of this point would require an elaborate modeling study which is beyond the scope of this paper. However, we would point out that in the simple six-energy level system presented in the Appendix, which provides an approximate description of the RT decay components, if the spectra associated with the antenna states (often known as species-associated spectra or SAS) are broad and asymmetric toward long wavelengths the negative amplitudes for the τ_2 DAS are absent. This is because they are masked by the positive, and numerically greater, amplitudes of the more blue-shifted absorbing states. Obviously, the assumption of spectrally broad and asymmetric states makes simple modeling schemes of this kind of limited accuracy.

In the discussion which follows, we will specifically address two aspects: first, that of slow spectral equilibration and its temperature sensitivity, based on analysis of the TRES, and second, that of the implications for diffusion- or trap-limited photochemistry.

The study presented here clearly demonstrates that two well-separated spectral equilibration processes (EP) can be detected in terms of the first central moment of the TRES. The faster (13−20 ps) precedes photochemical trapping and accounts for about 60−70% of the spectral shifting. This component is associated with spectral evolution from the bulk antenna toward the red forms, while the second, slow, component is associated with EP involving the low-energy spectral forms. To directly compare the total fluorescence decay due to reaction center trapping with the dynamics of spectral evolution, we have analyzed the first central moment of the time distribution of both processes. This type of analysis is useful as it allows a simple and direct comparison of the dynamics of the two processes without the necessity of performing elaborate model studies. It is clearly seen (Table 1) that both processes occur on a similar time scale at both 280 and 170 K. As the slow EP is largely associated with the red antenna forms, most of which are localized in the external antenna (LHCI; *30*), it is clear that antenna processes are a limiting factor in the overall rate of charge separation. We believe that this is the first clear demonstration of antenna spectral evolution occurring on a time scale similar to that of RC trapping.

The slow EP is mostly associated with a small number of low-energy chlorophyll forms, the excited states of which are strongly populated (more than 80% of the excited states) under steady-state illumination at room temperature (*2*). The importance of these red forms in the energy transfer pathway to P700 is once again underlined in this study as, from the integrated fluorescence decay in Figure 4, we estimate that only approximately 18−21% of the excited states are trapped during the first lifetime of the faster EP, involving bulk and red form transfer (τ = 20 ps at 170 K and 13 ps at 280 K) at these two temperatures, and between 40 and 50% during the first three lifetimes (Figure 4) when energy transfer into the red forms is virtually complete. This suggests that only a relatively small fraction of excited states are trapped after direct transfer from the bulk antenna to the core and P700, with more than half being trapped via the red forms. This aspect can be investigated using the kinetic model presented in the Appendix by determining the amount of reaction center trapping after setting the back transfer rates from the three low-energy levels (levels 4−6) equal to zero. In this way, we find that about 80% of the excited states are trapped only after transfer through the red forms, in close agreement with the steady-state fluorescence measurements (*2*) This conclusion is also in agreement with the recent studies of Savikhin et al. (*31*), who showed for the PSI core of *Synechocystis* that transfer to the red forms was faster than trapping.

It will be noted in the kinetic model (Appendix) that the different low-energy pigment "pools" are not directly coupled and hence may be envisaged as being dispersed in the "bulk" antenna. This conclusion is based on (i) the kinetic modeling of the fluorescence decay dynamics (Appendix). In the six-state scheme which we have used, it was found to be necessary to have the red pools uncoupled from each other; otherwise, decay from the red-most pools was too fast with respect to trapping and (ii) spectral evolution in the kinetic modeling of large heterogeneous pigment lattices is markedly biphasic, with a slow EP involving the red-most forms, only when these low-energy forms are not directly coupled (G. Zucchelli, A. Yu. Borisov, F. M. Garlaschi, R. C. Jennings, unpublished observation). This latter situation can also easily be simulated in simple three-state models (A−C) in which the two low-energy states (A and B) are either directly coupled or separated by the high-energy state (C). We therefore conclude that it is most probable that at least the 730 and 740 nm emitting spectral forms are spatially separated within the antenna and not organized in some kind of pigment cluster.

Detergent fractionation of this PSI-200 preparation (*30*) demonstrates that while some low-energy chlorophyll forms are present in the core, more than 80% are associated with LHCI, which also seems to account for the red-most absorbing forms, in agreement with other observations (*9*, *20*, *32*). Thus, the slow EP would seem to be associated with energy transfer processes occurring to a large extent in the external antenna.

The temperature sensitivity of spectral evolution is quite marked with a 3.4-fold decrease in the mean time upon

lowering the temperature from 280 to 170 K, and as pointed out above, this is mostly associated with the slow EP process. It is interesting to attempt to understand where this temperature effect occurs. In the theoretical framework of Förster theory, the effect of temperature is not explicitly considered. A temperature dependency however comes into the overlap integral term essentially as a donor−acceptor resonance modulation of the matrix interaction energy, taken over the entire zero−zero and vibronic energy spread. This effect was recently calculated by Zucchelli et al. (*36*) for chlorophyll bound to a chlorophyll−protein complex in the 150−300 K interval. Surprisingly, for downhill energy transfer, the temperature effect in the 300−150 K range was slight over the entire donor−acceptor energy gap that was considered (2200 cm^{-1}) and was almost zero for transfer from a bulk antenna chlorophyll (670−690 nm) to a red form (710−740 nm). This conclusion, based on a theoretical analysis, is supported by the temperature insensitivity in the 280−170 K interval reported here for the 10−11 ps transfer component (τ_1). On the other hand, calculations show that the uphill transfer rate is strongly temperature-dependent (*36*), as is expected from thermodynamic considerations. We therefore conclude that the quite large temperature effect on the slow EP demonstrates that this is almost exclusively associated with uphill transfer from the red forms to the bulk antenna chlorophylls, with almost no effect on downhill or isoenergetic transfer.

An important question concerning energy trapping in PSI and which has been frequently discussed in recent years (*15*, *22*, *33*, *34*) is whether this rate is controlled by energy diffusion within the antenna (diffusion-limited) or by the primary electron transfer processes which occur in the RC itself (trap-limited). A further possibility, known as transfer to trap-limited, was suggested by Valkunas et al. (*35*) which envisages transfer from the antenna to P700 as the limiting process. These possibilities may be summarized in terms of the following simple diagram, where A represents the antenna, C is some inner core chlorophyll molecules surrounding P700, P is P700, and P^+A^- is the primary charge separation state.

$$A \underset{k_{-1}}{\overset{k_1}{\rightleftharpoons}} C \underset{k_{-2}}{\overset{k_2}{\rightleftharpoons}} P \overset{k_3}{\rightleftharpoons} P^+A^-$$

In the diffusion limit, $k_1 < k_2$ and k_3. In the trap limit, $k_3 < k_1$ and k_2. In the transfer to trap case, $k_2 < k_1$ and k_3. As pointed out by White et al. (*33*), the relative values of the k_{-2} and k_3 processes are also important, and only in the case in which $k_3 \gg k_{-2}$ is a purely diffusion-limited case possible. While there is no clear evidence concerning the relative values of k_3, and k_{-2} for PSI, it is probable that significant back transfer from P to the near antenna molecules occurs (see the model in the Appendix), and thus, there will almost certainly be some degree of trap limitation. The important point thus becomes to determine whether the system is purely or largely trap-limited or whether there is a strong antenna (diffusional) effect. The dominant opinion concerning PSI is that it is largely trap-limited. This opinion is to a large extent based on the experimental detection of a 4−12 ps decay-associated spectral equilibration component in time-resolved fluorescence experiments which is many times faster than the excited-state decay due to RC trapping. Thus, trapping was thought to proceed from an essentially thermalized state, with energy flowing in and out of the primary donor many times prior to charge separation. In this paper, this view is to a certain extent contradicted as the overall antenna spectral evolution, as distinct from the bulk and red form transfer, is demonstrated to occur on a time scale similar to that of trapping. These data clearly point to an important effect of antenna processes on the overall trapping dynamics, a point of view which is supported by the rather similar temperature effect on spectral evolution and the mean overall trapping time (Table 1). We interpret this to indicate that the slow uphill energy transfer from the red forms to the bulk chlorophylls at 170 K, responsible for the temperature effect on antenna spectral evolution as discussed above, also slows the overall trapping rate. Any attempt to arrive at a more quantitative evaluation requires detailed modeling which is in principle possible with the six-state scheme presented in the Appendix. We would however prefer not to push such a simple model description of PSI too far and therefore refrain from presenting such an analysis.

APPENDIX

Kinetic modeling of PSI-200 was performed by numerically resolving, by the Laplace method, the six-differential equation system for the following six-state rate matrix. The numerical values provide a reasonable description of the fluorescence decay and steady-state parameters. However, as described in the Discussion, we stress that such a coarse-grained description is incapable of describing accurately the fine details of spectral evolution and is to be understood as an approximation.

rate matrix (ns^{-1})

	1	**2**	**3**	**4**	**5**	**6**
1	0.5	1200	0	103	38	12
2	120	0.5	3540	0	0	0
3	0	2000	2000	0	0	0
4	140	0	0	0.5	0	0
5	30	0	0	0	0.5	0
6	12	0	0	0	0	0.5

where **1** is the mean energy of the bulk antenna (685 nm, 180-fold degenerate), **2** is the group of six inner core chls (*4*) strongly coupled to P700 [for most calculations, this was at 695 nm (*2*) and was 6-fold degenerate], **3** is the P700 dimer (700 nm, 2-fold degenerate), and **4**−**6** are the three red forms (712 nm, 8-fold degenerate; 722 nm, 2-fold degenerate; 734 nm, 1-fold degenerate, respectively).

All energy levels are defined in terms or the approximate mean wavelength position of the absorption bands, and the ratio of each pair of rate processes is given by the population-weighted Boltzmann factor. The red forms are not directly coupled either with each other or with the inner core molecules. However, we note that our simulation results are not significantly altered if some coupling to the inner core is allowed.

This system has six eigenvalues, representing the decay lifetimes. The first two are on a femtosecond time scale and as such are not experimentally relevant. The third and fourth (3 and 19 ps, respectively) are too close to be readily resolved by the multicomponent fit routine. The fifth and sixth (50 and 130 ps, respectively) are close to the experimental values for the main decay components.

REFERENCES

1. Turconi, S., Weber, N., Schweitzer, G., Strotmann, H., and Holzwarth, A. R. (1994) *Biochim. Biophys. Acta 1187*, 324−334.
2. Croce, R., Zucchelli, G., Garlaschi, F. M., Bassi, R., and Jennings, R. C. (1996) *Biochemistry 35*, 8572−8579.
3. Jennings, R. C., Bassi, R., and Zucchelli, G. (1996) *Top. Curr. Chem. 117*, 147−181.
4. Krauss, N., Schubert, W.-D., Kuklas, O., Fromme, P., Witt, H. T., and Saenger, W. (1996) *Nat. Struct. Biol. 3*, 965−973.
5. Boekema, E. J., Boonstra, A. F., Dekker, J. P., and Rögner, M. (1990) *J. Bioenerg. Biomembr. 26*, 17−29.
6. Croce, R., and Bassi, R. (1998) in *Photosynthesis: Mechanisms and Effects* (Garab, G., Ed.) Vol. I, pp 421−424, Kluwer Academic Publishers, Dordrecht, The Netherlands.
7. Holzwarth, A. R., Schatz, G. H., Brock, H., and Bittersmann, E. (1993) *Biophys. J. 64*, 1813−1826.
8. Hastings, G., Keinherenbrink, A. M., Lin, S., and Blankenship, R. E. (1994) *Biochemistry 33*, 3185−3192.
9. Mullet, J. E., Burke, J. J., and Arntzen, C. J. (1980) *Plant Physiol. 65*, 814−822.
10. Wittmershaus, B. P., Berns, D. S., and Huang, C. (1987) *Biophys. J. 52*, 829−836.
11. Palsson, L.-O., Tjus, S. E., Andersson, B., and Gillbro, T. (1995) *Chem. Phys. 194*, 291−302.
12. Gobets, B., van Amerongen, H., Monshouwer, R., Kruip, J., Rogner, M., and van Grondelle, R. (1994) *Biochim. Biophys. Acta 1188*, 75−85.
13. Mukerji, I., and Sauer, K. (1989) in *Photosynthesis. Plant Biology* (Briggs, W. H., Ed.) Vol. 8, pp 105−122, Alan R. Liss, New York.
14. Karapetian, N. V., Dorra, D., Schweitzer, G., Beszmertnaya, I., and Holzwarth, A. R. (1997) *Biochemistry 36*, 13830−13837.
15. Turconi, S., Schweitzer, G., and Holzwarth, A. R. (1993) *Photochem. Photobiol. 57*, 113−120.
16. Turconi, S., Kruip, J., Schweitzer, G., Rogner, M., and Holzwarth, A. R. (1996) *Photosynth. Res. 49*, 263−268.
17. Palsson, L.-O., Dekker, J. P., Schlodder, E., Monshouwer, R., and van Grondelle, R. (1996) *Photosynth. Res. 48*, 239−246.
18. Owens, T. G., Webb, S. P., Alberte, R. S., Mets, L., and Fleming, G. R. (1988) *Biophys. J. 53*, 733−745.
19. Holzwarth, A. R., Scharz, G. H., Brock, H., and Bittersmann, E. (1983) *Biophys. J. 64*, 1813−1826.
20. Lam, E., Ortiz, W., Mayfield, S., and Malkin, R. (1984) *Plant Physiol. 74*, 650−655.
21. Hasting, G., Hoshina, S., Webber, A. N., and Blankenship, R. E. (1995) *Biochemistry 34*, 15512−15522.
22. Owens, T. G., Webb, S. P., Mets, L., Alberte, R. S., and Fleming, G. R. (1987) *Proc. Natl. Acad. Sci. U.S.A. 84*, 1532−1536.
23. van Metter, R. L., and Knox, R. S. (1976) *Chem. Phys. 12*, 333−340.
24. van Grondelle, R., Dekker, J. P., Gillbro, T., and Sundstrom, V. (1994) *Biochim. Biophys. Acta 1187*, 1−65.
25. Wendler, J., and Holzwarth, A. R. (1987) *Biophys. J. 52*, 717−728.
26. Holzwarth, A. R. (1997) in *Biophysical Techniques in Photosynthesis. Advances in Photosynthesis Research* (Amesz, J., and Hoff, A., Eds.) pp 75−92, Kluwer Academic Publishers, Dordrecht, The Netherlands.
27. Eadie, W. T., Drijard, D., James, F. E., Roos, M., and Sandoulet, B. (1971) *Statistical Methods in Experimental Physics*, North-Holland Publishing Co., Amsterdam and London.
28. Suter, G. W., Meister, E. C., and Wild, U. P. (1988) *SPIE 910*, 81−86.
29. Trinkunas, G., and Holzwarth, A. R. (1994) *Biophys. J. 66*, 415−429.
30. Croce, R., Zucchelli, G., Garlaschi, F. M., and Jennings, R. C. (1998) *Biochemistry 37*, 17355−17360.
31. Savikhin, S., Xu, W., Soukoulis, V., Chitnis, P. R., and Struve, W. S. (1999) *Biophys. J. 76*, 3278−3288.
32. Hawarth, P., Karukstis, K. K., and Sauer, K. (1983) *Biochim. Biophys. Acta 725*, 261−271.
33. White, N. T. H., Beddard, G. S., Thorne, J. R. G., Feehan, T. M., Keyes, T. E., and Heathcote, P. (1996) *J. Phys. Chem. 100*, 12086−12099.
34. Trissl, H.-W. (1997) *Photosynth. Res. 54*, 237−240.
35. Valkunas, L., Liuolia, V., Dekker, J. P., and van Grondelle, R. (1995) *Photosynth. Res. 42*, 149−154.
36. Zucchelli, G., Cremonesi, O., Garlaschi, F. M., and Jennings, R. C. (1998) in *Photosynthesis: Mechanisms and Effects* (Garab, G., Ed.) Vol. I, pp 449−452, Kluwer Academic Publishers, Dordrecht, The Netherlands.

BI992659R